

1     **Geometry and topology of Polish Outer Carpathian digital**  
2     **elevation model interpreted lineament network in context of**  
3                     **regional tectonics**

4     Maciej Kania<sup>1</sup>, Mateusz Szczęch<sup>1</sup>

5     <sup>1</sup>Jagiellonian University in Kraków, Faculty of Geography and Geology, Institute of Geological Sciences,  
6     Gronostajowa 3a, 30-863 Kraków, Poland

7     *Correspondence to:* Maciej Kania (maciej.kania@uj.edu.pl)

8

9 **Abstract.** The Polish part of the Western Outer Carpathians lineament network was analysed based on the  
10 GMTED2010 digital elevation model. Lineaments were identified in the visual screening of the hillshade model.  
11 To the best of our knowledge, no one has studied the geometrical properties of the network with relation to the  
12 topological ones. The NetworkGT QGIS toolbox was applied to identify the nodes and branches of the network,  
13 as well as to calculate the topology parameters. Our aim was to find differences between the western and eastern  
14 parts of the Western Outer Carpathians; therefore, the analyses were carried out in six sectors chosen based on  
15 the geographical subdivision in the geological context: three in the north, mainly the Silesian unit; and three in  
16 the south, mainly the Magura unit. We found general agreement of the identified network with the  
17 photolineament map; however, some of the photolineaments are not confirmed by digital elevation model  
18 (DEM). We found that the topological parameters of the networks change from west to east, but not from north  
19 to south. There are areas of increased interconnectivity, especially the Nowy Sącz Basin, where the lineament  
20 network may reflect a complicated system of cross-cutting deep-rooted fault zones in the basement.

## 21 1. Introduction

22 Remote sensing imagery is an important source of data in regional tectonics, and its importance has been  
23 growing in recent years. Since the 1970s, there have been multispectral satellite photos of the Earth surface  
24 applied mainly in mineral mapping (e.g. van der Meer et al., 2012), as well as in tectonic studies (e.g. Leech et  
25 al., 2003). The Shuttle Radar Topography Mission (SRTM) resulted in the first remote sensing digital elevation  
26 model of most of the continental surface of the planet, with immense potential for application in geology (Yang  
27 et al., 2011). Then, new superior resolution and quality models were created on both the global (satellite) and  
28 local scale (mainly airborne LiDAR scanning). Digital elevation models are especially useful in areas with lush  
29 vegetation. The application of LiDAR in the Carpathians' flysch-type mountains in geological interpretations  
30 was shown, for example, in Kania and Szczęch (2022).

31 Our previous study (Kania and Szczęch, 2020), based on the interpretation of the model augmented with field  
32 geological mapping (Szczęch and Cieszkowski, 2021), showed how a lineament network can be interpreted in  
33 topological and geometrical terms. ~~The aim in the present paper~~This paper presents is to up-scale DEM-based  
34 geometrical and topological analyses of a regional scale lineament network to find how this is reflected in the  
35 tectonic structure of the Western Carpathians. Previous studies of the Carpathian lineaments were mainly  
36 focused on lineament strikes distribution (e.g. Doktór and Graniczny, 1982, 1983; Doktór et al., 1985, 1990,  
37 2002; Bażyński et al., 1986; Graniczny and Mizerski, 2003); therefore, we decided to add an interconnectivity  
38 aspect in terms of the topological parameters (Valentini et al., 2007; Sanderson and Nixon, 2015; Thiele et al.,  
39 2016), as a way of better understanding the structural problems. Our aim was to find, if and how the deep-rooted  
40 lineaments (fault zones) are influencing lineament network pattern on the surface. Our hypothesis was that these  
41 deep-rooted features are expressed in the network independently of the contemporary observed Carpathian  
42 nappes stacked structure. Most of the Carpathian-related studies are geographically organised in mountain arc  
43 parallel belts, reflecting the main tectonostratigraphic units, now forming nappes and being sedimentary basins  
44 during the Carpathian flysch depositions. We decided to keep this subdivision, although combining this with  
45 physiographical subdivisions into sectors with borders perpendicular to the Carpathian belt.

## 2. Up-to-date Previous research on the Polish Outer Carpathian lineaments

The fact that dislocation lines perpendicular to the Carpathian arc are related to the deep basement, and are significantly older than the Carpathians themselves, was postulated even before the remote sensing era (Teisseyre, 1907). The first modern attempts to interpret lineaments in the Polish Carpathians were based on the Landsat MSS imagery and Heat Capacity Mapping Mission satellite, and reported together with data from the whole territory of Poland on a photogeological map at 1:1 000 000 scale (; Bażyński et al., 1986; Graniczny and Mizerski, 2003). The main lineament systems of the Western Carpathians in the context of structural geology were shown by Doktor and Graniczny (1983) and Doktor et al. (1985). The results of satellite imagery lineament detections were then correlated with geophysical data proving relationships between the surface, neotectonic processes and deep Carpathian basement structure (Motyl-Rakowska and Ślącza, 1984; Doktor et al., 1990). Airborne radar data were applied in tectonic analysis of the Carpathians, resulting in 17 000 short lineaments that were the basis of the lineament density map (Doktor et al., 2002). The interpretation of SRTM hillshading visualisation was performed by Chodyń (2004) on the limited area in Beskid Wyspowy Mts. Comparison of Landsat MSS and SRTM data by Ozimkowski (2008) showed that whilst the main faults can be related to lineaments, there are still numerous lineaments without geological explanation. [In the last few years LiDAR high resolution digital elevation models became available for the Polish Carpathians allowing more regional-scale lineament network analysis and their interpretation as fault-related features \(Kania and Szczęch, 2020, 2022; Szczęch and Cieszkowski, 2021; Barmuta et al., 2021; Sikora, 2022\)](#)

## 3. Study area

The choice of the study area was based on the physiogeographical subdivision of Poland by Solon et al. (2018). The following macroregions were selected: the Western Beskidy Foothills, Western Beskidy Mts., Orawa–Podhale Basin, Mid-Beskidy Foothills and Mid-Beskidy Mts (Fig. 1). These five regions, with a total area of 17 437 km<sup>2</sup>, cover most of the Polish part of the Outer Carpathians, excluding a small part of the Eastern Outer Carpathians located in Poland.

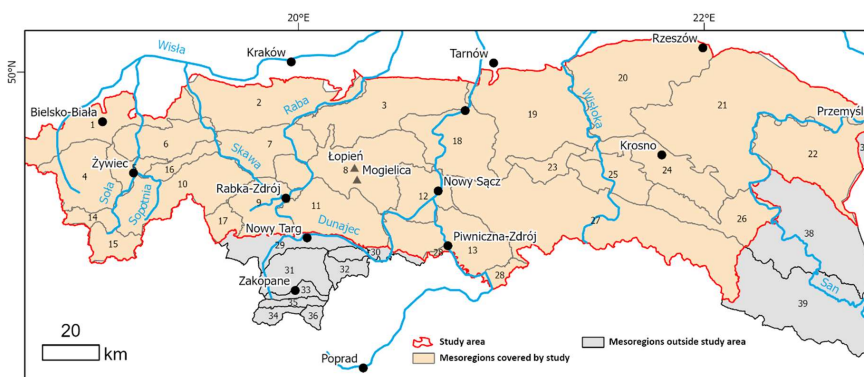


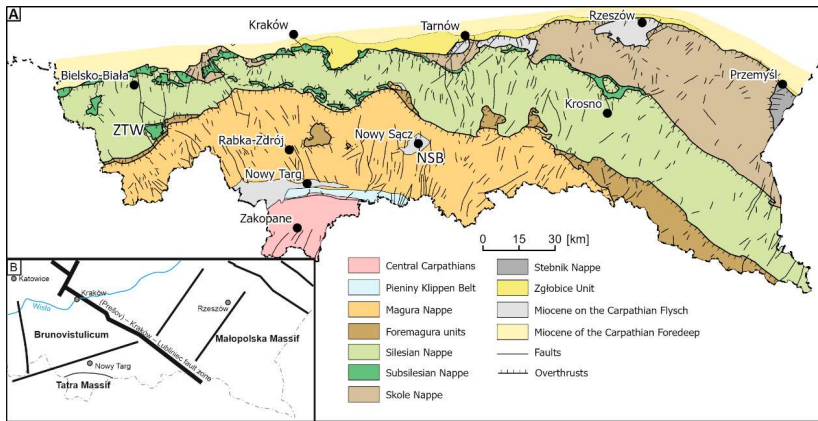
Fig. 1. Physiogeographical subdivision of the study area and adjacent parts of the Polish Carpathians based on Solon et al. (2018). Mesoregions covered by study: 1 – Silesia Foothills, 2 – Wieliczka Foothills, 3 – Wiśnicz Foothills, 4 – Silesian Beskid Mts, 5 – Żywiec Basin, 6 – Mały Beskid Mts, 7 – Makowski Beskid,

75 8 – Wyspowy Beskid, 9 – Orawa-Jordanów Foothills, 10 – Żywiec-Orawa Beskid Mts, 11 – Gorce Mts, 12  
76 – Sącz Basin, 13 – Sącz Beskid Mts, 14 – Koniaków Intermontane Region, 15 – Żywiec-Kysuce Beskid  
77 Mts, 16 – Pewel-Krzeczów Ranges, 17 – Orawa Interfluve, 18 – Rożnów Foothills, 19 – Ciężkowice  
78 Foothills, 20 – Strzyżów Foothills, 21 – Dynów Foothills, 22 – Przemyśl Foothills, 23 – Gorlice Basin, 24 –  
79 Jasło-Krosno Basin, 25 – Jasło Foothills, 26 – Bukowiec Foothills, 27 – Low Beskid Mts, 28 – Poprad  
80 Foothills; mesoregions outside the study area: 29 – Orawa-Nowy Targ Basin, 30 – Pieniny Mts, 31 – Fore-  
81 Tatra Foothills, 32 – Magura Spiska Mts, 33 – Sub-Tatra Depression, 34 – Western Tatra Mts, 35 –  
82 Regłowe Tatra Mts, 36 – High Tatra Mts, 37 – Hermanowice Submontane Region, 38 – Sanocko-  
83 Turczańskie Mts, 39 – Bieszczady Mts.

84

### 85 3.1 Geological setting of the study area

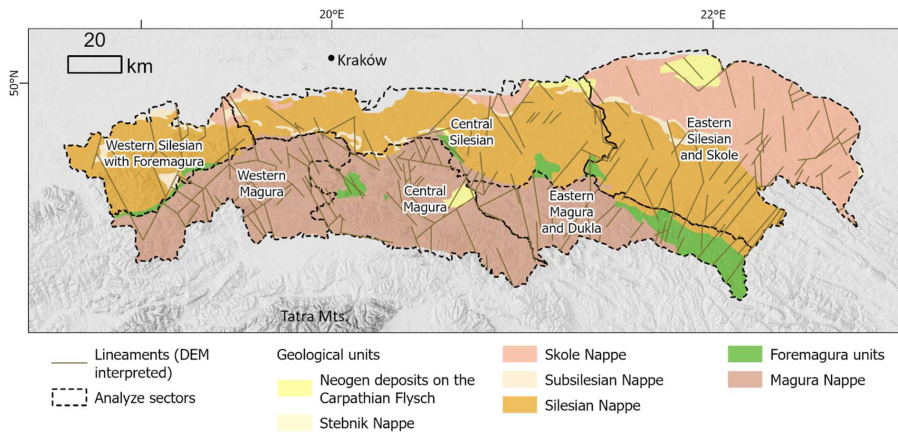
86 The research area is located in the Polish sector of the Western Outer Carpathians (Mahel', 1974; Książkiewicz,  
87 1977; Ślęczka et al., 2006; Fig. 2). It contacts tectonically with the Pieniny Klippen Belt from the south, which is  
88 a border between the Outer and the Central Carpathians (Książkiewicz, 1977; Plašienka, 2018; Golonka et al.,  
89 2019, 2021). The basement under the Western Outer Carpathians is formed of two blocks: Brunovistulicum and  
90 Małopolska Massif, which are separated by major tectonic zone: Kraków – Lubliniec Fault (Fig. 2B) Żaba, 1999;  
91 Żelaźniewicz, 2011), cut by numerous other deep rooted lineaments (Doktór, 1985). The Outer Carpathians are  
92 built mainly of flysch deposits, whose thickness is approximately 6 000 m, and thus they are also referred to as  
93 the Flysch Carpathians (Książkiewicz, 1977; Golonka et al., 2005, 2021; Ślęczka et al., 2006). These deposits are  
94 Late Jurassic–Early Miocene in age and are mainly deep-sea sediments deposited by the gravity flow in the  
95 several sedimentary basins of the Northern Tethys, separated by ridges (Książkiewicz, 1977; Golonka et al.,  
96 2005, 2021; Ślęczka et al., 2006). The thrust of the Central Carpathians block to the north on the European  
97 Platform blocks — the Brunovistulicum and Małopolska Massif (Żaba, 1999) — led to the forming of the  
98 synorogenic stage accretionary prism. The sediments deposited in the basins were folded and thrust one upon  
99 another, creating the sequence of the nappes in the Miocene. Going from the south there are the Magura Nappe,  
100 Dukla Nappe, Fore–Magura group of nappes, Silesian Nappe, Sub-Silesian Nappe and Skole Nappe (Mahel',  
101 1974; Książkiewicz, 1977; Golonka et al., 2005, 2019; Ślęczka et al., 2006). The deposits of the Outer  
102 Carpathians are overthrust on the Miocene molasses filling the Carpathian Foredeep, which was deposited on the  
103 front of the Outer Carpathian orogenic belt thrusting over the North European Platform (Ślęczka et al., 2006;  
104 Oszczytko, 2006).



105  
 106 **Fig. 2. A: Generalised geological map of the Polish part of the Carpathians based on Cieszkowski et al.,**  
 107 **2017 and cited there, faults after Lexa et al., 2000. B: Main tectonic units under the Carpathians, after**  
 108 **Żelaźniewicz et al., 2011.**  
 109

### 110 3.2 Analysis of the sectors

111 We used the morphometry subdivision of Poland (Solon et al., 2018) to define the area, based on the  
 112 subprovinces of the Western Outer Carpathians in the area of Poland and a small band of Northern Subcarpathia  
 113 subprovince to the border of the Carpathians in the geological meaning (Carpathian overthrust on the Foredeep  
 114 sediments), according to Lexa et al. (2000). The subdivision of the outer Carpathian belt is mostly used in the  
 115 geology basis on the tectonostratigraphic units (nappes). This subdivision, however, does not allow differences  
 116 in lineament systems parallel to the belt to be caught. The newly proposed morphostructural subdivision of the  
 117 Western Carpathians (Minár et al., 2011) is another approach that compiles geological and morphological  
 118 features. The Polish part of the Western Carpathians is subdivided into the following subregions (number  
 119 according to the paper cited): (3f) Moravian–Silesian Beskid, (3a) Beskid Żywiecki–Gorce, (3b) Beskid  
 120 Sądecki–Levočské vrchy, (5a) Beskid Wyspowy, (5b) Low Beskid and (6) North Foreland. The last subregion  
 121 spans all the length of the northern Carpathian boundary between the Orava and San rivers. We decided to  
 122 compile the geological subdivision with the morphological one (Solon et al., 2018), which also comprises a  
 123 subdivision of the outermost units, into five sectors (Fig. 3, Tab. 1). The only change was including Mount  
 124 Cicień in Beskid Wyspowy into the Central Silesian sectors, as this massif, unlike all other Beskid Wyspowy  
 125 culminations is built of Silesian series deposits (Burtan, 1974).



126  
127 **Fig. 3. Sectors defined based on the physiogeographical (Solon et al., 2018) and tectonic subdivisions**  
128 **(Golonka et al., 2021) of the study area (Western Outer Carpathians in Poland).**

129  
130 **Tab. 1. Analyse sectors**

Analyse sectors name;	Symbol	Mesoregions covered according to Solon et al., 2018
Western Silesian with Foremagura	WS	Silesian Beskid Mts., Żywiec Basin, Silesia Foothills, Mały Beskid Mts.
Central Silesian	CS	Wieliczka Foothills, Wiśnicz Foothills, Beskid Wyspowy Mts – only the Ciecień ridge, Rożnów Foothills, Ciężkowice Foothills, Gorlice Basin
Eastern Silesian and Skole	ES	Przemysł Foothills, Jasło-Krosno Basin, Strzyżów Foothills, Dynów Foothills, Jasło Foothills, Bukowiec Foothills
Western Magura	WM	Orawa-Jordanów Foothills, Orawa Interfluve, Koniaków Intermontane Region, Żywiec-Kysuce Beski, Pewel-Krzeczów Ranges, Makowski Beskid, Żywiec-Orawa Beskid
Central Magura	CM	Sącz Beskid Mts., Sącz Basin, Wyspowy Beskid (without Ciecień Ridge), Gorce Mts.
Eastern Magura and Dukla	EM	Low Beskid Mts.

131  
132 **4. Digital elevation model**  
133 The Global Multi-resolution Terrain Elevation Data 2010 (GMTED2010; see Danielson, 2011) 7.5 arc-second  
134 product was chosen as a work base. The model is a compilation of different raster-based elevation sources, based  
135 mainly on SRTM digital terrain elevation data. The resolution is ca. 0.0021°/pixel, which means ca. 233 m/pixel.

136 This was found to be sufficient, while the working scale during lineament detection was 1:150 000. As the  
137 shading azimuth can influence the results, the working imagery was multidirectional hillshade (Nagi, 2022).

## 138 **5. Methods**

### 139 **5.1 Multiple cover lineament detection**

140 The manual method of lineament extraction was applied for two reasons. First, it is the simplest, low cost and  
141 widely used method. The second reason is that it creates a basis for further work, based on automated extraction.  
142 However, the method used is prone to some operator-related bias (Scheiber et al., 2015; Ehlen, 2004). Thus, to  
143 reduce this bias the lineaments were extracted by two operators working independently, in three sessions,  
144 separated by intervals of several months. After each session, the results were analysed and a network of common  
145 features was created. Lineaments marked by both operators were merged into single feature. Lineaments marked  
146 by only one operator were removed. The last stage was creating a concise network of lineaments based on the  
147 results of the three sessions.

148

### 149 **5.2 Network analysis**

150 A network can be described by scale-independent topological characteristics, based on the case of a line network  
151 on graph theory. The network (graph) is formed by nodes (end or intersection points) connected by lines  
152 (Sanderson and Nixon, 2015; Mukherjee, 2019). The line can be formed by one or more branches connected by  
153 nodes. The node can be isolated (I type), an embranchment (Y type) or an intersection (X type), where the latter  
154 two types are connecting nodes. Thus, the branch can connect two I type nodes (I-I branch), isolated and  
155 connecting nodes (I-C branch, which can be I-Y or I-X) and two connecting nodes (C-C branch, which can be  
156 X-X, X-Y or Y-Y). The proportion of nodes and branch types can be analysed as tertiary systems that  
157 characterise the properties of the network, especially its interconnectivity (Procter and Sanderson, 2018;  
158 Sanderson and Nixon, 2015; Sanderson et al., 2018).

159 The spatial variation of the topological parameters of the network was analysed with the following aspects: (1)  
160 regular, in a 5x5 km grid; and (2) within sectors based on the mesoregions of physiogeographical subdivision,  
161 according to Solon et al. (2018) and the main tectonic units (Fig. 3 Tab. 1).

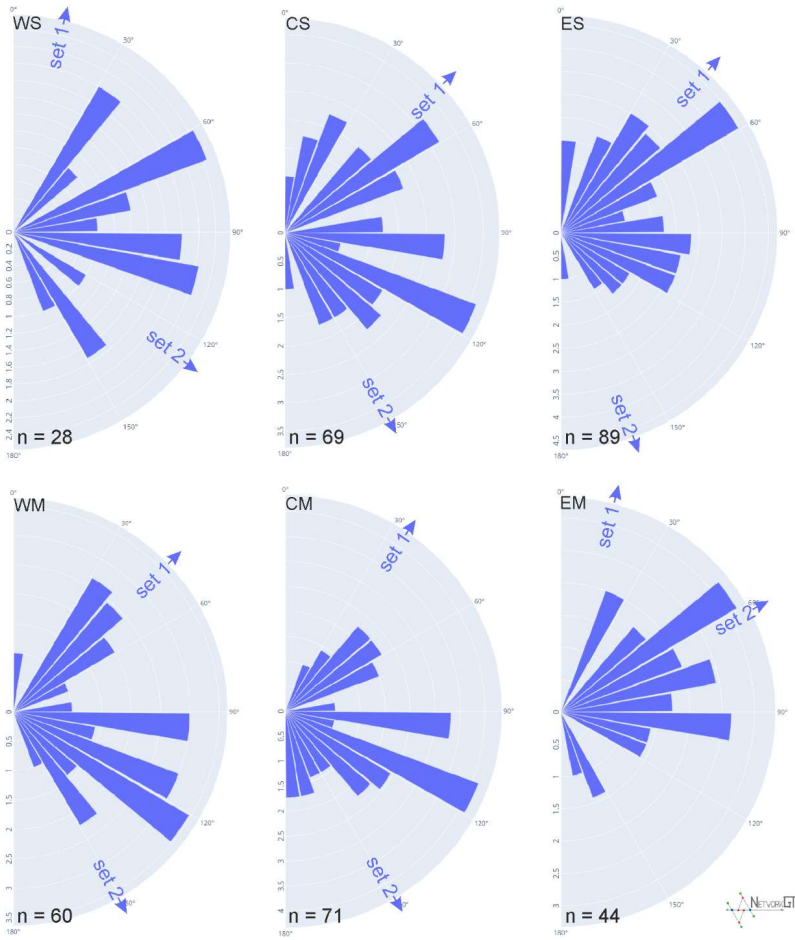
162 The NetworkGT Qgis toolbox (Nyberg et al., 2018) was used as a tool in the topological analyses. The lineament  
163 network was checked and repaired with NetworkGT tools. An additional stage was the manual correction of  
164 some features to eliminate all non-defined types of nodes, as well as some extremely short (ca. 500 m or shorter)  
165 features. The topological parameters were analysed in three modes: the whole network; the sectors defined; and  
166 in a regular, 5x5 km grid with 10 km search radius.

167 The Rayleigh test of semicircular distribution test was performed with the EZ-ROSE spreadsheet (Baas, 2000),  
168 and circular statistics were calculated with the SciPy stats module (The SciPy Community, 2022).

169 **6. Results**

170 **6.1 Network geometry**

171 The azimuths of the lineaments in all the analysed sectors show a multimodal distribution. Thus, the directions  
172 were separated into sets, in a way that gives low values of circular variance. The angular ranges of all the sets are  
173 presented in Tab. 2. For all sets, except for set 2 in the Eastern Magura (EM) sector and set 2 in the Western  
174 Silesian (WS) sector, the distribution is not uniform, as checked with the Rayleigh test (Baas, 2000). The two  
175 sets not checked were not numerous enough to be representative.



176 **Fig. 4: Rose diagrams of the analysed networks in the analytic sectors; upper row: Western Silesian sector**  
177 **with Foremagura (WS), Central Silesia (CS), Eastern Silesia with Skole (ES); lower row: Western Magura**  
178 **(WM), Central Magura (CM), and Eastern Magura with Dukla (EM). Arrows mark the mean azimuth for**  
179 **the sets defined in Tab. 2.**

181



182 **Tab. 2. Azimuths of the lineaments in the analyse sectors**

Analyse sector	Set	Azimuths range	n	Circular statistics			The acute angle between sets means
				Mean	Std. dev	Variance	
CS	1	0 – 100	15	46.5	14.2	3.5	75.5
	2	100 – 180	13	151	16.6	4.8	
CM	1	0 – 80	17	34.1	13	3	63.9
	2	80 – 180	51	150.2	21.5	8.1	
EM	1	45 – 75	41	62.1	7.5	1.0	47.7
	2	0 – 45 75 – 180	3	14.4	26.7	12.5	
ES	1	0 – 100	59	42.7	19.7	6.8	62.1
	2	100 – 180	28	160.6	14.7	3.8	
WM	1	0 – 100	20	46.5	14.2	3.5	75.5
	2	100 – 180	40	151	16.6	4.8	
WS	1	0 – 60 150 – 180	23	13.6	23.3	9.5	66.2
	2	60 – 150	5	127.4	8.9	1.4	

183  
 184 The orientation of lineaments in all sectors, as well as the circular mean azimuth are shown in Fig. 4. In sectors  
 185 Central and Eastern Silesian (CS, ES) and Central and Western Magura (CM, WM) the set 1 mean is located  
 186 between 34° and 47°, marking a dominant SW–NE strike of lineaments. In the Western Silesian sector (WS), set  
 187 1 is oriented more to the north (14°). In all sectors above, there is a second set with a NW–SE trend, mostly  
 188 oriented at 150–160°, but in the Western Silesian sector case the mean azimuth is lower (127°), as in the case of  
 189 the first set. The last sector, Eastern Magura and Dukla, is different. There is one dominant set with azimuth 62°,  
 190 and the second set is poorly represented and oriented northward. The angle between the two sets varies in the  
 191 62–76° range, except in the Eastern Magura and Dukla sector where it is only 48°.

192 **6.2 Network topology**

193 In the study area, 305 lineaments were marked in total. These features comprise 432 nodes. Of this count, 58%  
 194 are I nodes, 19% are E nodes, 18% are Y nodes and 5% are X nodes. The network contains 338 branches, within  
 195 which 49% are C–I type branches, 29% are C–C branches and 22% are I–I branches marking completely  
 196 separated lineaments. Topological parameters are shown in Tab. 3.

197  
 198 **Tab. 3. Topological parameters of the network in analyse sectors**

	Western Silesian with Foremagura	Central Silesian	Eastern Silesian and Skole	Western Magura	Central Magura	Eastern Magura and Dukla	Whole area

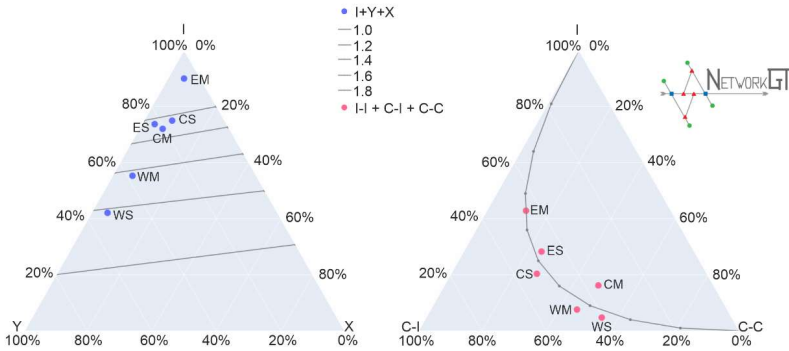
	WS	CS	ES	WM	CM	EM	
No. of nodes (I+X+Y)	19	68	101	47	67	40	383
I nodes	8	51	76	26	48	36	293
X nodes	1	6	6	3	6	2	19
Y nodes	10	11	21	18	15	2	71
E nodes	22	38	49	46	61	52	-
C-C connections	11.5	14.5	18.5	21.0	33.5	3.0	77.0
C-I connections	8.5	28.5	35.5	22.0	25.0	11.5	131.0
I-I connections	1.0	11.0	23.5	3.0	14.0	10.5	81.0
No. of branches	21.0	54.0	77.5	46.0	54.5	25.0	291
No. of lines	9.0	31.0	48.5	22.0	31.5	19.0	182
No. of connections	11	17	25	21	19	4	90
Connects per line	2.44	1.10	1.03	1.91	1.21	0.42	0.99
Connects per branch	1.62	1.06	1.02	1.43	1.12	0.56	0.99
Dim.less intensity	1.21	0.87	1.21	1.65	1.33	2.06	0.75
Av. Degree of network	2.21	1.59	1.53	1.96	1.63	1.25	1.52

199

200

201 The highest dimensionless intensity parameter is in the Eastern Magura and Dukla sector (2.05) and the lowest in  
202 the Central Silesian (0.87). On the other hand, the Eastern Magura sector is characterised by the lowest  
203 connections per branch (0.56) or the average degree of network (1.25) due to its form of mainly parallel features,  
204 with only 12% of the branches of connecting type (C–C). The best interconnectivity is observed in the Western  
205 Silesian sector with 1.62 connections per branch and an average degree of the network of 2.21. This is an effect  
206 of the presence of the Żywiec Basin block-system in the central part of the region.

207 The difference between these two (Eastern Magura and Western Silesia) sectors can be clearly visible on the  
208 ternary diagrams (Fig. 5) presenting the relationships of the nodes and branch types. In the Western Silesian  
209 sector, there is a high ratio of Y type nodes (52% of non-E-type nodes) and only one I–I branch.



210 **Fig. 5: Ternary diagram presenting nodes (left) and branches (right) proportions in the analyse sectors.**

211  
212  
213 The parameters of all the other sectors fall between the Eastern Magura and Western Silesian sectors. The  
214 Western Magura sector has quite good interconnectivity with a similar type of Eastern Magura blocky network.  
215 Another approach to analysing topology is to use a sampling regular grid. The results are shown in Fig. 5 as  
216 maps of connections per branch number, 2D network intensity and dimensionless intensity.

217 It can be seen we have two relatively large regions with a high value of connections per branch parameter . The  
218 first one is in the Western Silesian and partially Western Magura sectors, that is, the Żywiec Basin area, but from  
219 the geological point of view it is also a narrow zone of Foremagura units occurring between the Silesian and  
220 Magura nappes. Moreover, the Subsilesian unit tectonic window occurs in this area.

221 The Nowy Sącz Basin (eastern part of the Central Magura sector in the subdivision used here) is the next region  
222 with a high number of connections per network branch. The lineament system in this area surrounds a zone of  
223 Neogene deposits lying on the Carpathian flysch and filling the intramountain Nowy Sącz Basin.

224 The 2D intensity map shows that the Nowy Sącz Basin is characterised in general by a higher intensity than the  
225 Żywiec Basin. There is also a general trend of higher intensity in the western part of the Carpathians (especially  
226 the Western Magura and Central Magura sectors) than in the eastern part (Eastern Magura and Dukla).

227 In terms of dimensionless intensity parameter there are two regions with significantly high values: the south-  
228 eastern part of the Wiśnicz foothill, which is in the Central Silesian sector, and the eastern parts of the Beskid  
229 Niski Mts. and Bukowiec foothill in the Eastern Magura and Eastern Silesian sectors, on the geographical border  
230 of the Western and Eastern Carpathians.

231 **7. Discussion**

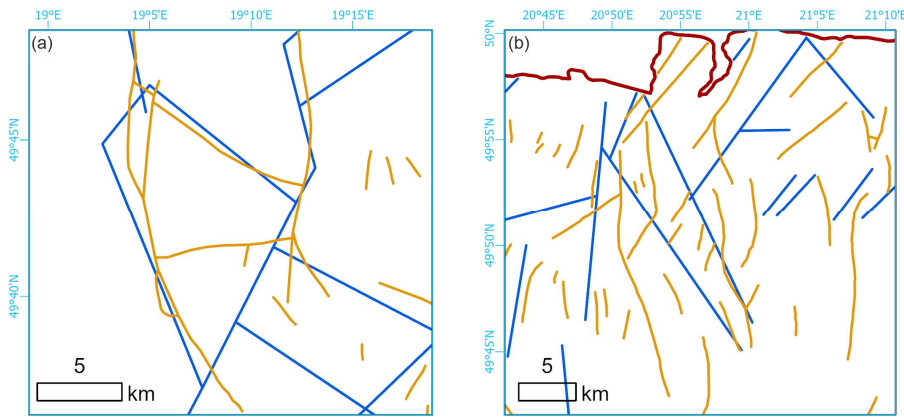
232 **7.1 Different lineament identification approaches**

233 There are 110 photolineaments marked on the photogeological map of Poland in the studied area (Bażyński et  
234 al., 1986). In the same area of the geological map of the Carpathians, Lexa et al. (2000) marked 2 325 features  
235 described as a fault or assumed fault. In many cases, our lineament system seems to be concordant or  
236 complimentary to Lexa et al.'s (Fig. 6). In some cases, the features marked as faults are rather thrust lines, as per  
237 the Fig. 6a example. The photolineament system is in general concordant with the DEM-interpreted system.

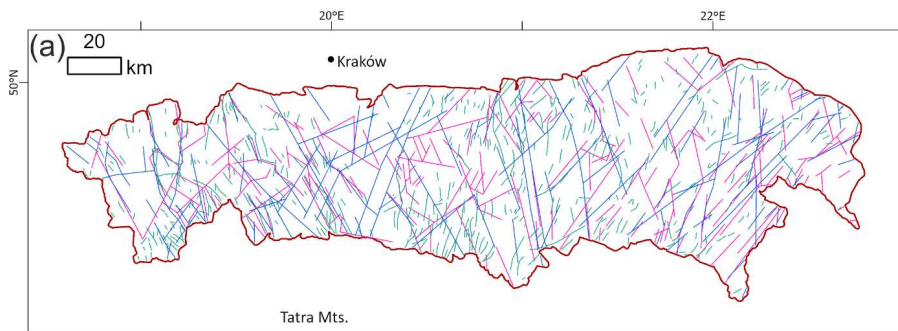
238 Visual inspection of the compiled lineaments map (Fig. 7a) shows that the especially NE striking lineaments of

239 the Eastern Magura sector are consistent with each other. Moreover, the system framing the Żywiec tectonic  
 240 window is well visible in both sets. On the other hand, there are some photolineaments that are not recognisable  
 241 on the DEM, and in fact also hardly visible on the modern orthophoto map. The most prominent example are two  
 242 straight, parallel lineaments striking the NNE in the central part of the study area, cutting its entire width. These  
 243 features seem to cut Gorcze Mts.; this is not confirmed by our other studies (Kania and Szczęch, 2020; Szczęch  
 244 and Cieszkowski, 2021). Further to the north, these two lineaments are delimiting massifs of the Beskid  
 245 Wyspowsy Mts. (Mogieliica, Łopień). These massifs are in fact particularly visible on the aerial photo, as rather  
 246 isometric 'islands', and are formed by core parts of the synclines (Wójcik et al., 2009). On the other hand, some  
 247 lineament systems well visible in DEM are not marked on the photolineament map, as per the case of the system  
 248 north of the Nowy Sącz. That shows how these two methods can in fact be recognised as complementary  
 249 approaches to the lineaments' identification.

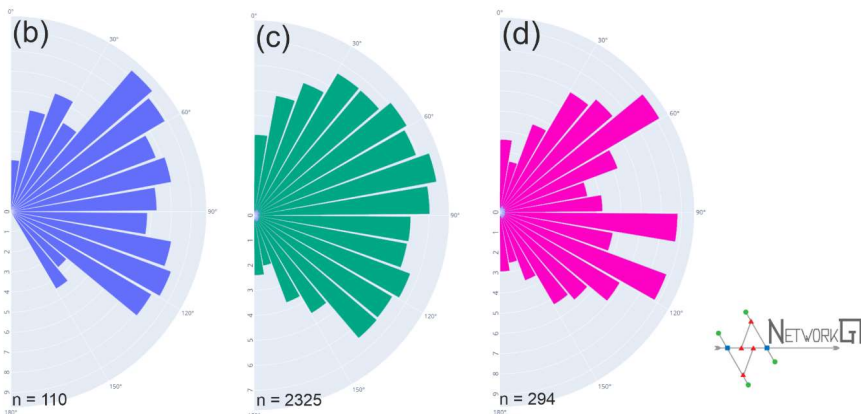
250 The system from the map by Lexa et al. (2000) shows confirmed and inferred faults, which is why it is not fully  
 251 compatible with lineaments; the lineaments, even when mainly tectonic related, are in fact a broader term  
 252 (O'Leary et al., 1976). Especially, these data, despite being a very rich collection of features are not applicable  
 253 for topological analyses: most of the features are short and isolated even when forming a network. Nevertheless,  
 254 these data include faults that are identified with geological criteria that are not visible in the remote sensing (at  
 255 least at the scale applied in this paper or by Bażyński et al., 1986 photolineament map. These data are  
 256 augmenting each other, which is highly visible in the Piwniczna Zdrój area, where DEM interpreted that the  
 257 NNW striking lineament along the Poprad River Valley (not present in the photolineament set) is flanked with a  
 258 set of N or NNE striking faults, which we have not identified on the DEM.



259  
 260 **Fig. 6. Comparison of lineament system detected from the GMETD model (blue) and faults by Lexa et al.,**  
 261 **2000 (brown). (a) Żywiec Basin area, (b) fragment of the Zakliczyn – Olszyny fault zone.**



— Photolineaments by Bażyński et al., 1986    — Faults by Lexa et al., 2000    — Lineaments (DEM interpreted)



262  
 263 **Fig. 7. Geometry of lineament networks in the Carpathians. (a) compilation map of lineaments by**  
 264 **Bażyński et al., 1986, faults by Lexa et al., 2000 and lineaments interpreted from DEM in the presented**  
 265 **paper. (b-d) rosedigrams of features azimuth in the whole study area from: (b) Bażyński et al. (1986), (c)**  
 266 **Lexa et al., 2000 and (d) DEM interpreted.**

267  
 268 When analysing the distribution of feature azimuth for the whole study area (Fig. 7b-d), it can be noted that the  
 269 directions for the photolineament set (B) and DEM-interpreted set (D) are quite similar. What is noteworthy is  
 270 the lack of azimuths greater than 150° in the photo set, which are present (albeit in a minority) in the DEM set.  
 271 Furthermore, the photo set shows two maxima, at ca. 45° and 110°, whilst in the DEM set there are three  
 272 maxima at ca. 50°, 100° and 110°. However, the dominating directions are not in fact distributed uniformly  
 273 along the W–E span of the Polish Western Carpathians, which can be clearly seen in Fig. 7a where the  
 274 domination of NE directions in the eastern sectors can be noticed, as well as the presence of two main directions  
 275 in the western and central sectors.

276 **7.2 Dominating directions of the lineament network**

277 We observed a difference in dominating azimuths of lineaments between the western/central sectors (WS, WM,  
278 CS, CM) and eastern sectors (ES, EM) of the study area. The first ones are characterised by two distinct sets of  
279 lineaments (NNE or NE and SE), while the second has an SE set that is strongly reduced.

280 According to the general tectonic model of the Outer Carpathians (Unrug, 1980), the flysch deposits are cut by  
281 set sinistral strike-slip fault zones. These fault zones are arranged in a fan-like shape along the arc of the  
282 Carpathians, leading to the rotation of the set of nappes (Unrug, 1980; Graniczny and Mizerski, 2003). The  
283 observed trend of increasing importance of the NE direction to the east is consistent with this model. However,  
284 the more complicated geometry of the western part of the network may be related to the more complicated  
285 system of the deep-rooted fault zones in this part (see further discussion below).

286 **7.3 Topological differentiation of the network**

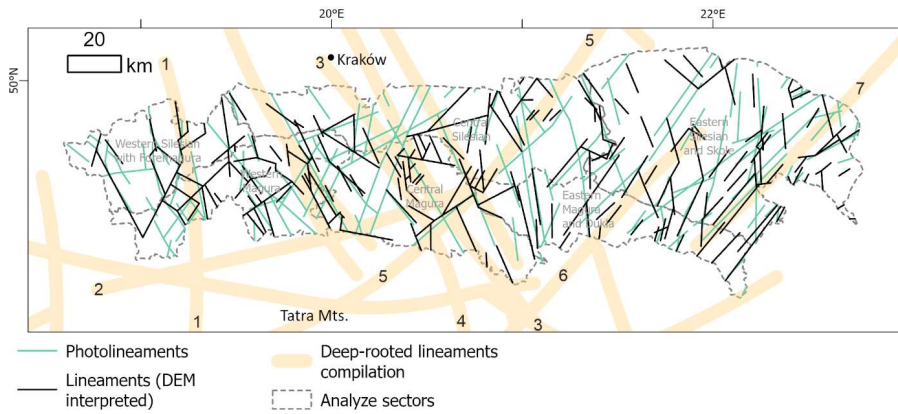
287 There are no topological analyses of the lineament networks for the Outer Carpathians. Our previous article  
288 (Kania and Szczęch, 2022) was focused on one mountain massif: Gorce Mts. From the tectonic point of view,  
289 this massif is quite homogenous, being located in the one tectono-facial unit (Magura unit) with some subunits  
290 within (Bystrica and Krynica subunits). Therefore, the paper focused mainly on different lithostratigraphic units,  
291 showing how different types of lithology differ in topology terms.

292 Scaling the research into the Polish Western Carpathians shows that in general there are no differences in the  
293 network topology related to the tectono-facial units (Outer Carpathian nappes) since in general, all these units are  
294 similar in lithology (flysch packets). However, there are differences related to some irregularities in tectonics:  
295 especially, the intramountain basins are marked with increased network interconnectivity. The western part of  
296 the study area in general has a better developed network. Especially, the Eastern Magura differs from the rest of  
297 the sectors: the domination of one lineament direction results in low network interconnectivity, which is  
298 expressed by a high proportion of the I nodes and I-I branches (Fig. 5). We analysed Magura unit and part of  
299 the Dukla unit together; however, the interconnectivity in the Dukla Nappe (belonging to the Foremagura group)  
300 is stronger than in Magura, which can be related to the proximity of the Silesian unit overthrust.

301 The highest interconnectivity was observed in the Western Silesian sector. The area is characterised by a high  
302 proportion of Y nodes, and thus mainly by the presence of C-I or C-C branches (Fig. 5). In the geological  
303 context, it is related to the location of the Żywiec tectonic window, which exposes the Subsilesian unit.  
304 However, the topological study shows that the tectonised zone is wider; the increase in connections per branch  
305 zone continues to the south along the Soła River and further, at least to the state border in the Beskid Żywiecki  
306 Mts.

307 **7.4 Main large-scale, deep-rooted lineament systems of the Western Carpathians and their**  
308 **relation to DEM-interpreted lineaments**

309 The following, well-known, large-scale lineaments reach the Carpathian basement cutting the Polish part of the  
310 Outer Western Carpathians (Doktór et al., 1985): Central Slovakia, Myjava, Muran, Štítik and Przemyśl. There  
311 are also lineaments not named by Doktór et al. (1985), but striking parallel, approximately 10 km to the east  
312 from the Skawa fault zone (Cieszkowski et al., 2006). Fig. 8 presents the generalised positions of the lineaments.



313  
 314 **Fig. 8. Interpreted lineament system with photolineaments by Bażyński et al., 1986 as well as deep-rooted**  
 315 **lineament compilation after Sikora, 1976; Zuchiewicz, 1984; Doktor et al., 1985. Important deep-rooted**  
 316 **lineaments mark with numbers: 1 – Central Slovakia, 2 – Pericarpathian, 3 – Kraków – Prešov, 4 –**  
 317 **Štítnik, 5 – Myjava, 6 – Muran, 7 - Przemysł**

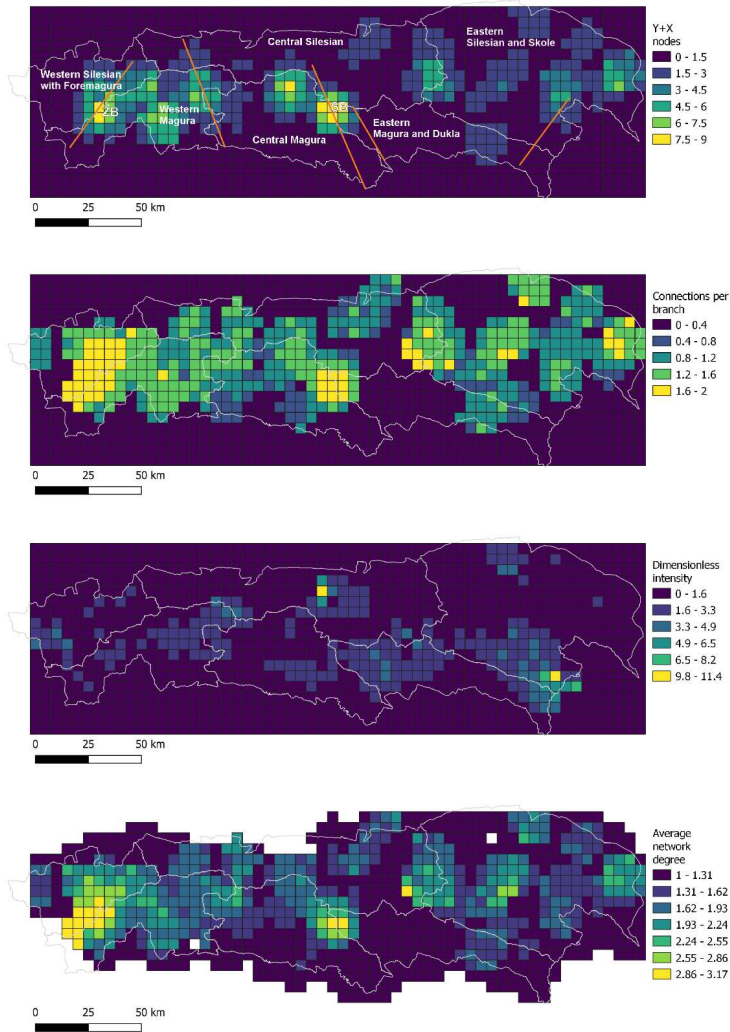
318  
 319 The central Slovak line marks the eastern border of the Żywiec basin and marks the major fault zone well visible  
 320 in the displacing Fore-Magura belt near Żywiec. Some of the lineaments belonging to the system can also be  
 321 traced to the east, with some connecting NE-SW branches near the northern margin of the Carpathians.

322 The system of Muran lineaments in the discussed region is marked by a few short NE-SW lineaments in the  
 323 eastern sectors of the Magura and Silesian units. The Myjava system, in fact one of the most prominent systems  
 324 in the Carpathians, in the study area can be traced along the Nowy Sącz Basin, continuing to the north where  
 325 there is a series of short lines parallel to the zone lineaments. The network interconnectivity increases in this  
 326 area. The lineaments there lie in an extension of the Carpathian Shear Corridor, a large-scale strike-slip zone  
 327 between Vienna and the High Tatra Mts. (Marko et al., 2017). Although the Štítnik system is unclear, some  
 328 parallel or subparallel lineaments can be assigned to this zone. The Przemysł lineament zone is identified as a set  
 329 of long lineaments in the easternmost parts of the area, where the main features of NE-SW are possibly  
 330 interconnected by shorter N-S lines, forming an interconnected, blocky, two-set system.

331 Another important deep-rooted linear structure, confirmed by a negative gravimetric anomaly is the  
 332 Pericarpathian line, which runs along the Nowy Sącz-Nowy Targ-Kysucké Nové Mesto line (Zuchiewicz, 1984;  
 333 Sikora, 1976), which runs similarly to the Myjava structure. The Kraków-Prešov lineament, which is an  
 334 extension of the Kraków-Lubliniec fault zone and marks the border between the Małopolska and  
 335 Brunovistulicum blocks of the basement (Žaba, 1999; Zuchiewicz, 1984). A system of lineaments is clearly  
 336 visible along this line, mainly in the Magura Nappe; however, parallel photolineaments were marked even longer  
 337 to the north (Bażyński et al., 1986).

338  
 339 These systems can be arranged in two sets: NNW, NW-SSE, SE striking (Central Slovakia, Skawa, Kraków-  
 340 Presov and Štítnik); and NE-SE (Myjava and Pericarpathian, Muran and Przemysł). That implies some points of  
 341 system intersection, and in the area analysed such a place is in the Nowy Sącz region. This place is characterised

342 by higher interconnection factors (Fig. 9), in relation to the surrounding area. Moreover, in terms of  
 343 geomorphology, this is an intramountainous basin, being the only location where deposits are observed in the  
 344 Magura Nappe Neogene.



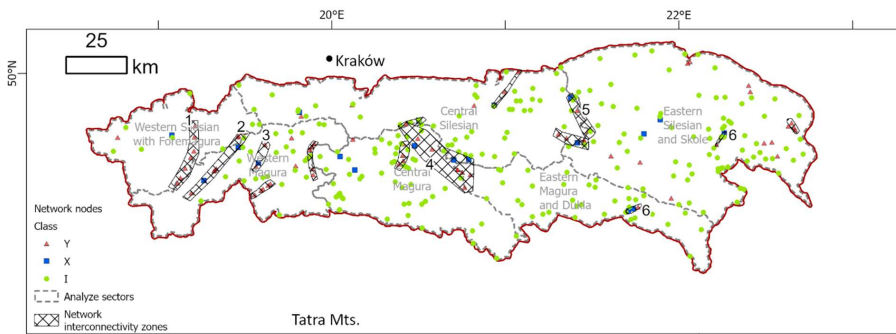
345  
 346  
 347 **Fig. 9. Topological parameters of the lineament network, from up to down: connecting nodes number,**  
 348 **connections per branch number, dimensionless intensity factor, and average network degree. ZB – Żywiec**  
 349 **Basin (Żywiec tectonic window), SB – Nowy Sącz Basin, lines on X-Y nodes map are main faults.**  
 350



351 The Central Slovakian system strikes along the east border of the Żywiec Basin and Żywiec tectonic window,  
 352 where the Subsilesian Nappe is exposed. We also marked a major lineament there, which is not present on the  
 353 photolineament map (Bażyński et al., 1986) or the database of the Western Carpathian Geological Map (Lexa et  
 354 al., 2000). The lineament (in the central part, the Soła River Valley) cuts the Magura Nappe, the Foremagura  
 355 zone with Magura overthrust and the Silesian Nappe. This structure is one of the edges of the rhomboidal block,  
 356 in which the Żywiec Basin has been developed. The generally increased degree of network interconnection (Fig.  
 357 10) and the intensity of the network in this area can be an effect of the interaction between the central Slovakian  
 358 system with the Soła lineament and all the lowered block edges.

359 The cross-cutting relations of the Myjava lineament and the Štitník lineament, whose continuation can be the  
 360 Dunajec fault system, are reflected in the bimodality of lineaments. The dominating maximum in the central  
 361 Magura sector, at approximately 120°, is similar to the Štitník lineament; however, the Myjava lineament is  
 362 reflected there by just a few dominating lineaments, which are relatively long. Moreover, the Pericarpathian  
 363 lineaments are also known in this region. This structure, reflected in the sedimentary cover as the Dunajec fault  
 364 zone, is also confirmed by a negative gravimetric anomaly (Zuchiewicz, 1984; Sikora, 1976). Another deep  
 365 structure cutting this area is the Kraków–Prešov fault, which is an extension of the Kraków–Lubliniec fault zone  
 366 under the Carpathians active to the Quaternary (Żaba, 1999). All these deep cross-cutting features result in an  
 367 increased degree of the network connectivity observed on the surface. Then, the blocky structure allowed the  
 368 formation of an intramountain basin, filled with Neogene sediments.

369 Topological analysis also suggests that the well-known Skawa fault zone (Zuchiewicz et al., 2009; Unrug, 1980)  
 370 is in fact the western-most part of the wider zone of increased network interconnectivity, extending ca. 10–20 km  
 371 to the west of the Raba River. The final interpretation of correlation of lineaments increased interconnectivity  
 372 areas with tectonic structures of the area is shown on the Fig. 10.



373 **Fig. 10. Network nodes and zones of interconnectivity and their interpretation in context of Outer**  
 374 **Carpathians Nappes (surface) and basement (deep) tectonics. 1 – Soła fault zone (surface), Central**  
 375 **Slovakia lineament (deep), 2 – fault system along Sopotnia Valley, 3 – Skawa fault zone (surface), 4 –**  
 376 **Nowy Sącz Basin (surface), Kraków – Prešov, Myjava and Štitník lineaments (deep), 5 – faults along**  
 377 **Wisłoka Valley (surface), 6 – Muran lineament (deep).**

379  
 380 The other aspect of the fault system of the Carpathians is occurrence and migration of the mineral waters. The  
 381 area to the south of the Nowy Sącz there is a well-known region of CO<sub>2</sub>-rich mineral waters occurrence with

382 renowned spa sites. These waters are associated with fault zones, often the deep one, penetrating to the  
383 crystalline basement of the Carpathians (Oszczypko and Zuber, 2002; Zuber and Chowaniec, 2009; Ciężkowski  
384 et al., 2010). Its noteworthy, that this region is located on the crossing of two major deep-rooted fault zones:  
385 Śtítník lineament and Myjava lineament (Fig. 8). Similarly, the deep faults can be patch of migration of  
386 hydrocarbons, especially if source rocks are related to the platform cover of Brunovistulicum and Małopolska  
387 Massif lying under the Carpathians. In fact, some of the Polish Carpathian gas deposits are related to the  
388 Mesozoic-Palaeozoic basement (Kotarba and Koltun, 2006). Thus, the analyse of the fault systems and their  
389 interconnectivity has the potential in study of both, hydrocarbon and hydrogeological systems.

## 390 7.5 Conclusions

391 The proposed data source and analysis method are complementary with other lineament analysis from the study  
392 area. The observed azimuths are in general concordant with the photolineament network; however, there are  
393 some structures that are not confirmed by DEM interpretation. The relationship between the DEM-interpreted  
394 data and geologically confirmed faults shows the usefulness of DEM as a data source in fault detection.

395 The dominating directions of the network are typical for the Western Carpathians, with a clear increase of the  
396 NE striking features proportion towards the east.

397 The topological properties of the lineament network in the Western Carpathians show E–W trends, but no clear  
398 S–N (perpendicular to the tectonic units) trends. This justifies the proposed subdivision of the Carpathians in the  
399 western, central and eastern sectors in addition to the tectono-facial subdivision. The eastern sectors are  
400 dominated by NE–SW trends and low interconnectivity, while the central and western sectors are more  
401 interconnected and characterised by cross-cutting relationships of two main lineament directions. The degree of  
402 network interconnectivity increases in areas with a lower morphology (intramountainous basins): the Żywiec  
403 Basin and Nowy Sącz Basin.

404 The geometry of the network, in general, reflects a system of deep-rooted lineaments. The cross-cutting area of  
405 the main deep lineaments is reflected in stronger network interconnectivity in the Nowy Sącz area.

406 CrediT authorship contribution statement: Maciej Kania: Conceptualization, Methodology, Formal analysis,  
407 Investigation, Writing – original draft, Visualization. Mateusz Szczęch: Investigation, Writing – review &  
408 editing, Visualization.

409  
410 Declaration of competing interest: The authors declare that they have no known competing financial interests or  
411 personal relationships that could have appeared to influence the work reported in this paper  
412  
413

414 Acknowledgements: The research was financed from funds of the Jagiellonian University Institute of  
415 Geological Sciences. Proofreading of this publication has been supported by a grant from the Priority Research  
416 Area (Digiworld) under the Strategic Programme Excellence Initiative at Jagiellonian University. The authors  
417 would like to thank both referees, Prof. Fabrizio Balsamo and Prof. Jan Golonka for their helpful comments  
418 improving a quality of the paper.

## 419 References

420 Baas, J. H.: EZ-ROSE: a computer program for equal-area circular histograms and statistical analysis of two-  
421 dimensional vectorial data, *Computers & Geosciences*, 26, 153–166, [https://doi.org/10.1016/S0098-](https://doi.org/10.1016/S0098-3004(99)00072-2)  
422 [3004\(99\)00072-2](https://doi.org/10.1016/S0098-3004(99)00072-2), 2000.

423 [Barmuta, J., Starzec, K., and Schnabel, W.: Seismic-Scale Evidence of Thrust-Perpendicular Normal](#)

— sformatowano: Angielski (Zjednoczone Królestwo)

424 [Faulting in the Western Outer Carpathians, Poland, Minerals, 11:1252, https://doi.org/10.3390/min11111252,](https://doi.org/10.3390/min11111252)  
425 [2021.](https://doi.org/10.3390/min11111252)

426 Bażyński, J., Doktor, S., and Graniczny, M.: Mapa fotogeologiczna Polski w skali 1:1 000 000, 1986.

427 Burtan, J.: Detailed Geological Map of Poland, 1:50 000 scale, Mszana Dolna sheet. Wydawnictwa Geologiczne,  
428 Warszawa, 1974.

429 Chodyń, R.: Zastosowanie cyfrowego modelu terenu (DEM) w badaniach geologicznych na przykładzie obszaru  
430 między Dobczycami a Mszaną Dolną (polskie Karpaty zewnętrzne), *Przegląd Geologiczny*, 52, 315–320, 2004.

431 Cieszkowski, M., Golonka, J., Waškowska-Oliwa, A., and Chrustek, M.: Budowa geologiczna rejonu Sucha  
432 Beskidzka – Świnna Poręba (polskie Karpaty fliszowe), *Geologia / Akademia Górniczo-Hutnicza im. Stanisława*  
433 *Staszica w Krakowie*, 32, 155–201, 2006.

434 Cieszkowski, M., Kysiak, T., Szczęch, M., and Wolska, A.: Geology of the Magura Nappe in the Osielec area  
435 with emphasis on an Eocene olistostrome with metabasite olistoliths (Outer Carpathians, Poland), *Annales*  
436 *Societatis Geologorum Poloniae*, 87, 169–182, <https://doi.org/10.14241/asgp.2017.009>, 2017.

437 Ciężkowski, W., Chowaniec, J., Górecki, W., Krawiec, A., Rajchel, L. and Zuber, A.: Mineral and thermal  
438 waters of Poland, *Przegląd Geologiczny*, 58, 762–773, 2010.

439 Danielson, J. J.: Global Multi-resolution Terrain Elevation Data 2010 (GMTED2010) Coastal Elevation  
440 Modeling View project LP DAAC View project, 2011.

441 Doktor, S. and Graniczny, M.: Geologiczna interpretacja zdjęć satelitarnych i radarowych wschodniej części  
442 Karpat, *Kwartalnik Geologiczny*, 26, 231–245, 1982.

443 Doktor, S. and Graniczny, M.: Fotogeologiczna analiza zdjęć satelitarnych Karpat, *Kwartalnik Geologiczny*, 27,  
444 645–656, 1983.

445 Doktor, S., Dornic, J., Graniczny, M., and Reichwalder, P.: Structural elements of Western Carpathians and their  
446 Foredeep on the basis of satellite interpretation, *Geological Quarterly*, 29, 129–138, 1985.

447 Doktor, S., Graniczny, M., Kucharski, R., Molek, M., and Dąbrowska, B.: Wgłębna budowa geologiczna Karpat  
448 w świetle kompleksowej analizy teledetekcyjno-geofizycznej, *Przegląd Geologiczny*, 38, 469–475, 1990.

449 Doktor, S., Graniczny, M., Kowalski, Z., and Wójcik, A.: Możliwości zastosowania wyników interpretacji zdjęć  
450 radarowych do analizy tektonicznej Karpat, *Przegląd Geologiczny*, 50, 852–860, 2002.

451 Ehlen, J.: Lineation, edited by: Goudie, A. S., *Encyclopedia of Geomorphology*, 2, 623–624, 2004.

452 Golonka, J., Aleksandrowski Paweł and Aubrecht, R., Chowaniec, J., Chrustek, M., Cieszkowski, M., Florek, R.,  
453 Gawęda, A., Jarosiński, M., Kępińska, B., and others: The Orava deep drilling project and post-palaeogene  
454 tectonics of the northern Carpathians, *Annales Societatis Geologorum Poloniae*, 75, 211–248, 2005.

455 Golonka, J., Waškowska, A., and Ślęczka, A.: The Western Outer Carpathians: Origin and evolution, *Zeitschrift*  
456 *der Deutschen Gesellschaft für Geowissenschaften*, 229–254, 2019.

457 Golonka, J., Gawęda, A., and Waśkowska, A.: Carpathians, Reference Module in Earth Systems and  
458 Environmental Sciences, in: Alderton, D. and Elias, S. A. (eds.): Encyclopedia of Geology (Second Edition),  
459 Academic Press, 372–381, <https://doi.org/10.1016/b978-0-12-409548-9.12384-x>, 2021.

460 Graniczny, M. and Mizerski, W.: Lineamenty na zdjęciach satelitarnych Polski – próba podsumowania, *Przegląd  
461 Geologiczny*, 51, 474–482, 2003.

462 Kania, M. and Szczęch, M.: Geometry and topology of tectonolineaments in the Gorze Mts. (Outer Carpathians)  
463 in Poland, *J Struct Geol*, 141, 104186, <https://doi.org/10.1016/j.jsg.2020.104186>, 2020.

464 Kania, M. and Szczęch, M.: Tectonic Structures Interpretation Using Airborne-Based LiDAR DEM on the  
465 Examples from the Polish Outer Carpathians, in: Atlas of Structural Geological and Geomorphological  
466 Interpretation of Remote Sensing Images, edited by: Misra, A. A. and Mukherjee, S., 157–165, 2022.

467 Kotarba, M.J. and Koltun, Y.V.: The Origin and habitat of hydrocarbons of the Polish and Ukrainian parts of the  
468 Carpathian Province, in: Golonka, J. and Picha, F., *The Carpathians and Their Foreland: Geology and  
469 Hydrocarbon Resources: AAPG Memoir*, 84, 321–368, 2006.

470 Książkiewicz, M.: The Tectonics of the Carpathians, in: *Geology of Poland*, vol. 4. Tectonics. The Alpine  
471 Tectonic Epoch, Geological Institute, Warszawa, 476–608, 1977.

472 Leech, D. P., Treloar, P. J., Lucas, N. S., and Grocott, J.: Landsat TM analysis of fracture patterns: A case study  
473 from the Coastal Cordillera of northern Chile, *Int J Remote Sens*, 24, 3709–3726,  
474 <https://doi.org/10.1080/0143116031000102520>, 2003.

475 Lexa, J., Bezák, V., Elečko, M., Mello, J., Polák, M., and Vozár, J.: Geological map of western Carpathians and  
476 adjacent areas 1:500 000, 2000.

477 Mahel', M.: Tectonics of the Carpathian–Balkan Regions, Explanations to the Tectonic Map of the Carpathian-  
478 Balkan Regions and Their Foreland., Štátny geologický ústav Dionýza Štúra, Bratislava, 180–197 pp., 1974.

479 Marko, F., Andriessen, P. A. M., Tomek, Č., Bezák, V., Fojtíková, L., Bošanský, M., Piovarči, M., and  
480 Reichwalder, P.: Carpathian Shear Corridor – A strike-slip boundary of an extruded crustal segment,  
481 *Tectonophysics*, 703–704, 119–134, <https://doi.org/10.1016/j.tecto.2017.02.010>, 2017.

482 Van der Meer, F. D., van der Werff, H. M. A., van Ruitenbeek, F. J. A., Hecker, C. A., Bakker, W. H., Noomen,  
483 M. F., van der Meijde, M., Carranza, E. J. M., de Smeth, J. B., and Woldai, T.: Multi- and hyperspectral geologic  
484 remote sensing: A review, <https://doi.org/10.1016/j.jag.2011.08.002>, 2012.

485 Minár, J., Bielik, M., Kováč, M., Plašienka, D., Barka, I., Stankoviansky, M., and Zeyen, H.: New  
486 morphostructural subdivision of the Western Carpathians: An approach integrating geodynamics into targeted  
487 morphometric analysis, *Tectonophysics*, 502, 158–174, 2011.

488 Motyl-Rakowska, J. and Ślęczka, A.: Ważniejsze lineamenty Karpat i ich związek ze znanymi uskokami,  
489 *Przegląd Geologiczny*, 32, 72–77, 1984.

490 Mukherjee, S.: Using Graph Theory to Represent Brittle Plane Networks, 259–271,  
491 <https://doi.org/10.1016/B978-0-12-814048-2.00022-3>, 2019.

492 Nagi, R.: Introducing Esri's Next Generation Hillshade: [https://www.esri.com/arcgis-blog/products/arcgis-](https://www.esri.com/arcgis-blog/products/arcgis-living-atlas/imagery/introducing-esri-next-generation-hillshade/?rmedium=redirect&rsource=blogs.esri.com/esri/arcgis/2014/07/14/introducing-esri-next-generation-hillshade)  
493 [living-atlas/imagery/introducing-esri-next-generation-](https://www.esri.com/arcgis-blog/products/arcgis-living-atlas/imagery/introducing-esri-next-generation-hillshade/?rmedium=redirect&rsource=blogs.esri.com/esri/arcgis/2014/07/14/introducing-esri-next-generation-hillshade)  
494 [hillshade/?rmedium=redirect&rsource=blogs.esri.com/esri/arcgis/2014/07/14/introducing-esri-next-generation-](https://www.esri.com/arcgis-blog/products/arcgis-living-atlas/imagery/introducing-esri-next-generation-hillshade/?rmedium=redirect&rsource=blogs.esri.com/esri/arcgis/2014/07/14/introducing-esri-next-generation-hillshade)  
495 [hillshade](https://www.esri.com/arcgis-blog/products/arcgis-living-atlas/imagery/introducing-esri-next-generation-hillshade/?rmedium=redirect&rsource=blogs.esri.com/esri/arcgis/2014/07/14/introducing-esri-next-generation-hillshade), last access: 1 June 2022.

496 Nyberg, B., Nixon, C. W., and Sanderson, D. J.: NetworkGT: A GIS tool for geometric and topological analysis  
497 of two-dimensional fracture networks, *Geosphere*, 14, 1618–1634, <https://doi.org/10.1130/GES01595.1>, 2018.

498 O'Leary, D. W., Friedman, J. D., and Pohn, H. A.: Lineament, linear, lineation: Some proposed new standards  
499 for old terms, *Geological Society of America Bulletin*, 87, 1463–1469, 1976.

500 Oszczytko, N.: Late Jurassic-Miocene evolution of the Outer Carpathian fold-and-thrust belt and its foredeep  
501 basin (Western Carpathians, Poland), *Geological Quarterly*, 50, 169–194, 2006.

502 Oszczytko, N. and Zuber, A.: Geological and isotopic evidence of diagenetic waters in the Polish Flysch  
503 Carpathians. *Geologica Carpathica*, 53, 257–268, 2002.

504 Ozimkowski, W.: Lineamenty otoczenia Tatr - porównanie interpretacji DEM i MSS, *Przegląd Geologiczny*, 56,  
505 1099–1102, 2008.

506 Plašienka, D.: Continuity and episodicity in the early Alpine tectonic evolution of the Western Carpathians: How  
507 large-scale processes are expressed by the orogenic architecture and rock record data, *Tectonics*, 37, 2029–2079,  
508 2018.

509 Procter, A. and Sanderson, D. J.: Spatial and layer-controlled variability in fracture networks, *J Struct Geol*, 108,  
510 52–65, <https://doi.org/10.1016/j.jsg.2017.07.008>, 2018.

511 Sanderson, D. J. and Nixon, C. W.: The use of topology in fracture network characterization, *J Struct Geol*, 72,  
512 55–66, <https://doi.org/10.1016/j.jsg.2015.01.005>, 2015.

513 Sanderson, D. J., Peacock, D. C. P., Nixon, C. W., and Rotevatn, A.: Graph theory and the analysis of fracture  
514 networks, *J Struct Geol*, 14th April, <https://doi.org/10.1016/j.jsg.2018.04.011>, 2018.

515 Scheiber, T., Fredin, O., Viola, G., Jarna, A., Gasser, D., and Łapińska-Viola, R.: Manual extraction of bedrock  
516 lineaments from high-resolution LiDAR data: methodological bias and human perception, 137, 362–372,  
517 <https://doi.org/10.1080/11035897.2015.1085434>, 2015.

518 Sikora, W.: On lineaments found in the Carpathians, *Rocznik Polskiego Towarzystwa Geologicznego*, 46, 3–37,  
519 1976.

520 [Sikora, R.: Geological and geomorphological conditions of landslide development in the Wisła source area of the](https://doi.org/10.7306/gq.1651)  
521 [Silesian Beskid mountains \(Outer Carpathians, southern Poland\), \*Geological Quarterly\*, 66: 19,](https://doi.org/10.7306/gq.1651)  
522 <http://dx.doi.org/10.7306/gq.1651>, 2022.

523 Ślęczka, A., Kruglov, S., Golonka, J., Oszczytko, N., and Popadyuk, I.: Geology and hydrocarbon resources of  
524 the Outer Carpathians, Poland, Slovakia, and Ukraine: general geology, in: Golonka, J. and Picha, F., *The*  
525 *Carpathians and Their Foreland: Geology and Hydrocarbon Resources: AAPG Memoir*, 84, 221–258, 2006.

526 Solon, J., Borzyszkowski, J., Małgorzata Bidłasik, Richling, A., Badora, K., Balon, J., Brzezińska-Wójcik, T.,  
527 Chabudziński, Ł., Dobrowolski, R., Grzegorzczak, I., Jodłowski, M., Kistowski, M., Kot, R., Krąż, P., Lechnio,

528 J., Macias, A., Majchrowska, A., Malinowska, E., Migoń, P., Myga-Piątek, U., Nita, J., Papińska, E., Rodzik, J.,  
529 Strzyż, M., Terpiłowski, S., Ziaja, W., and Paul, J.: Physico-geographical mesoregions of Poland: verification  
530 and adjustment of boundaries on the basis of contemporary spatial data, *Geographia Polonica*, 91, 143–170,  
531 <https://doi.org/10.7163/GPol.0115>, 2018.

532 Szczęch, M. and Cieszkowski, M.: Geology of the Magura Nappe, south-western Gorce Mountains (Outer  
533 Carpathians, Poland), *Journal of Maps*, 17, 453–464, <https://doi.org/10.1080/17445647.2021.1950579>, 2021.

534 Teisseyre, W.: O związku w budowie tektonicznej Karpat i ich przedmurza, *Kosmos*, 32, 393–402, 1907.

535 Statistics (scipy.stats) — SciPy v1.9.3 Manual: <https://docs.scipy.org/doc/scipy/tutorial/stats.html>, last access: 8  
536 November 2022.

537 Thiele, S. T., Jessell, M. W., Lindsay, M., Ogarko, V., Wellmann, J. F., and Pakyuz-Charrier, E.: The topology  
538 of geology 1: Topological analysis, *Journal of Structural Geology*, 91, 27–38,  
539 <https://doi.org/10.1016/J.JSG.2016.08.009>, 2016.

540 Unrug, R.: Tectonic rotation of flysch nappes in the Polish Outer Carpathians, *Rocznik Polskiego Towarzystwa*  
541 *Geologicznego*, 50, 27–39, 1980.

542 Valentini, L., Perugini, D., and Poli, G.: The “small-world” topology of rock fracture networks, *Physica A:*  
543 *Statistical Mechanics and its Applications*, 377, 323–328, <https://doi.org/10.1016/j.physa.2006.11.025>, 2007.

544 Wójcik, A., Czerwiec, J., and Krawczyk, M.: Szczegółowa Mapa Geologiczna Polski 1:50 000. arkusz  
545 Limanowa, 2009.

546 Yang, L., Meng, X., and Zhang, X.: SRTM DEM and its application advances,  
547 <https://doi.org/10.1080/01431161003786016>, 2011.

548 Zuber, A. and Chowaniec, J.: Diagenetic and other highly mineralized waters in the Polish Carpathians, *Applied*  
549 *Geochemistry*, 24, 1889–1900, 2009.

550 Zuchiewicz, W.: The late Neogene - Quaternary tectonic mobility of the Polish West Carpathians - a case study  
551 of the Dunajec drainage basin, *Annales Societatis Geologorum Poloniae*, 54, 133–189, 1984.

552 Zuchiewicz, W., Tokarski, A. K., Świerczewska, A., and Cuong, N. Q.: Neotectonic Activity of the Skawa River  
553 Fault Zone (Outer Carpathians, Poland), *Annales Societatis Geologorum Poloniae*, 79, 67–93, 2009.

554 Żaba, J.: Ewolucja strukturalna utworów dolnopaleozoicznych w strefie granicznej bloków górnośląskiego i  
555 małopolskiego, *Prace Państwowego Instytutu Geologicznego*, 166, 1–162, 1999.

556 Żelaźniewicz, A., Aleksandrowski, P., Buła, Z., Kornkowski, P. H., Konon, A., Oszczytko, N., Ślącza, A.,  
557 Żaba, J. and Żytka, K.: Regionalizacja Tektoniczna Polski. Komitet Nauk Geologicznych PAN, Wrocław, 1–60  
558 pp., 2011.

559  
560